Journal of Entomology and Zoology Studies

Available online at www.entomoljournal.com

E-ISSN: 2320-7078
P-ISSN: 2349-6800
JEZS 2018; 6(2): 1976-1986

Received: 07-01-2018
Accepted: 08-02-2018

Ahmed HF AL-Bayati
Department of Surgery and Obstetrics / College of Veterinary Medicine/University of Baghdad-Iraq

Falah Mahmood Hameed
1) Department of Surgery and Obstetrics / College of Veterinary Medicine/University of Baghdad-Iraq
2) Department of Surgery and Obstetrics College of Veterinary Medicine, University of kerbala-Iraq

Correspondence
Ahmed HF AL-Bayati
Department of Surgery and Obstetrics / College of Veterinary Medicine/University of Baghdad-Iraq

Effect of acellular bovine pericardium and dermal matrixes on cutaneous wounds healing in male rabbits: Histopathological evaluation

Ahmed HF AL-Bayati and Falah Mahmood Hameed

Abstract
The present study was designed to evaluate the effects of two types of natural materials (Biomaterials), acellular bovine pericardium (BP) and acellular dermal matrix (ADM) on full-thickness cutaneous wounds healing in male rabbits. The animals were housed in metal cages in the animal house of the Veterinary Medicine College, Baghdad University, along the period of the study 35days from 4 March to 10 April of 2017. A total of seventy five (2X2) centimeters of square full-thickness cutaneous wounds were created in 50 male rabbits under the effect of I/M administration of a mixture of 5mg/kg of xylazine hydrochloride and 35mg/kg of ketamine hydrochloride. The dorsal aspects (back) of lateral thoracic side of animals were prepared for aseptic surgery. Two wounds were made on one side of the back, the caudal one as treatment wounds, and the cranial as control wounds with a distance of (5-7) cm between each. Depending on the method of the treatment, these wounds were divided into three groups (A, B and C) (25 wounds/group). In group (A), the caudal wounds were treated immediately by covering of wound bed with a sheet of ADM, and in group (B), the wounds were treated by covering of wounds bed with a sheet of BP, while in group (C), the cranial wounds were left without treatment, as a control wounds. For histopathological evaluation, each group was divided into five subgroups (five wounds/subgroup). The histopathological studying on (3, 7, 14, 21 and 35) days post-treatment revealed that BP, ADM treated wounds have enhanced cellularity, increased vasculature than those in untreated wounds. Depending on the histopathological findings, this study confirms that local implantation of xeno-grafting BP and ADM leads to enhance and develop of cutaneous wound healing.

Keywords: acellular bovine pericardium (BP), acellular dermal matrix (ADM), cutaneous wounds, rabbit, wounds healing

1. Introduction
The skin protects the body from the outer environment by homeostasis and maintaining temperature in addition to performing immune observation and sensory detection [1]. Cutaneous wound healing is a highly arranged and coordinated sequence of processes lead to return of tissue functions and integrity. An disorder in the regular wound healing process may lead to the progress of non-healing chronic wounds. Many of factors may lead to a delay in wound healing including diabetes, renal disease, trauma, venous or arterial insufficiency and old age [2]. In addition to local factors such as; ischemia, tissue hypoxia, foreign bodies, exudates, infection, maceration of tissue, distraction of the regulation of the inflammatory process and systemic factors like; immune status or compromised nutritional can all weaken healing [3,4].
There are a variety of treatment methods suitable including; wound dressings [5], compression bandaging [6], ultrasound [7], negative pressure wound therapy [8], debridement [9] and skin substitutes [10], which can be costly, time consumption and may be slow to prove any true results. In spite of the great number of treatment options, still present regimes are not enough, as these injuries remain an important economic load and a clinical problem [11]. So, there is an essential need to accelerate the healing for acute and chronic wounds with improve the healing of wounds and the restoration of damaged tissue to a point that is not currently possible with normal care measures or newly progressing innovative approaches.
Recently, the using of biologic scaffold materials for a different of applications has increased dramatically through the last two decades [12]. Biologic scaffolds resulting from decellularized organs and tissues have been successfully used in together human clinical applications and in pre-clinical animal studies [13]. After remove of cells from the tissue, they produce a complex

mixture of structural and functional proteins that formation the extracellular matrix (ECM). ECM can be harvested from the different tissues, the species of source and the decellularization protocols for these biologic scaffolds differ widely [14, 15], explained that ECM which can be getting from heart valves, nerves, tendons, blood vessels, ligaments, small intestine submucosa (SIS), skeletal muscle and urinary bladder sub-mucosa (UBM), have been used for regenerative medicine and tissue engineering applications.

The common of biomaterials resulting from biological sources have high protein content that can be used to provide some attractive characteristics [16]. Bovine pericardium (BP) and ADM are rich in collagen containing commonly type-I, as well as glycosaminoglycans (GAGs) and glycoproteins, growth factors, cytokines and chemokines [17, 18, 19]. There have been little of studies that investigate the role of ECM on healing process of tissues and concerning for their clinical success mainly for BP and ADM. Therefore, the objectives of the current study was to assess and compare histopathological between BP and ADM effects as a natural biological scaffolds, as a sheet, on healing of full thickness cutaneous wounds.

2. Materials and Methods

The present study was occurr in the animal house of the Veterinary Medicine College, Baghdad University, along the period of the study 35days from 4 March to 10 April of 2017.

2.1 Experimental Animals

Fifty (50) healthy adult local breed male rabbits weighting (1-2) kg, were recruited for this study. All animals were evaluated clinically by a physical examination before initiation of the experiments. The animals were housed in metal cages (30x70x60) cm in an air-conditioned room in the animal house of the Veterinary Medicine College, Baghdad University, along the period of the experiment, receiving free accesses to water and food (Pellets). The animals were left for four weeks for adaptation with experimental condition and injections of anti-coccidiosis drug were used.

2.2 Surgical operation

A total of seventy five of (2X2) centimeters of square full-thickness cutaneous wounds were created in 50 male rabbits under the effect of I/M administration of a mixture of 5mg/kg of xylazine hydrochloride and 35mg/kg of ketamine hydrochloride.

The animals were secured in ventral recumbency and the dorsal aspect (back) of lateral thoracic side of animal was prepared for aseptic surgery. Two wounds were made on one side of the back, the caudal one as treated wound, and the cranial as control wound (untreated wounds) with a distance of (5-7) cm between each one. These wounds were allocated, depending on the method of the treatment, into three groups (A, B and C) (25 wounds/group). In group (A), the caudal wounds were treated immediately by placing and covering of wound bed with a sheet of ADM, and in group (B), the wounds will be treated by placing and covering of wounds bed with a sheet of BP, while, in group (C), the cranial wounds were left without treatment, as a control group.

2.3 Preparation of bovine pericardium extracellular matrix (BP-ECM)

Bovine pericardium was obtained from the local abattoir, immediately after slaughtering. Then, the pericardium was submerged in phosphate buffered saline (PBS) in order to be transported to the laboratory. The tissue gently rinsed with PBS to get rid of the adhered blood. Mechanical cleaning was performed manually to eliminate all unwanted fat and connective tissue from the pericardium using dry gauze. Then, decellularized with (0.1) peracetic acid (PAA) and (4%) ethanol combination for two hours and cleaned with PBS and deionized water for 15 minutes. The prepared a cellular BP linked tissue matrices was stored at 4°C in PBS containing 1% Gentamycin [20, 21].

2.4 Preparation of Acellular Dermal Matrix (ADM)

Bovine skin was decellularized as described by [22], with some modifications. In brief, the skin of bovine origin was collected from the local abattoir and immediately preserved in ice-cold sterile PBS (pH7.4) containing a broad spectrum antibiotic and 0.25% of ethylenediaminetetraacetic acid (EDTA). In laboratory, the specimens were shaved and washed by sterile PBS to remove all the adherent blood and debris. The skin was de-epithelialized using 0.25% trypsin and 2M sodium chloride solution for eight hours. After de-epithelialization, the dermis was decellularized using 2% sodium deoxycholate for 48 hours. The samples were subjected to continuous agitation in a horizontal orbital shaker at the rate of 180 (rotations/min) during de-epithelialization and decellularization process to provide better contact of tissue with chemicals. Following decellularization, the prepared ADM was washed six times (2 hours each) with sterile PBS to remove the residual chemicals and stored in PBS solution containing antibiotic solution at-20°C.

2.5 Histopathological evaluation

The histopathological evaluation was performed on day (3, 7, 14, 21 and 35) post-treatment with BP and ADM and the same period was depended for the control group (five wounds / period). A full-thickness incisional biopsy specimens were obtained (5-6) mm in width and they included approximately (3-4) mm of unwounded skin on both sides of the wound which were fixed in (10%) neutral formalin solution, and then embedded in paraffin which were followed by sectioned in (5-7) micron on a rotary microtome and staining with hematoxylin-eosin (H&E) and Van-Giessen stains [23].

2.6 Statistical Analysis

The Statistical Analysis System-SAS [24] was used to effect on different factors (treatment & days) in study parameters (percentage). The least significant difference (LSD) test was used to comparative between percentages in this study.

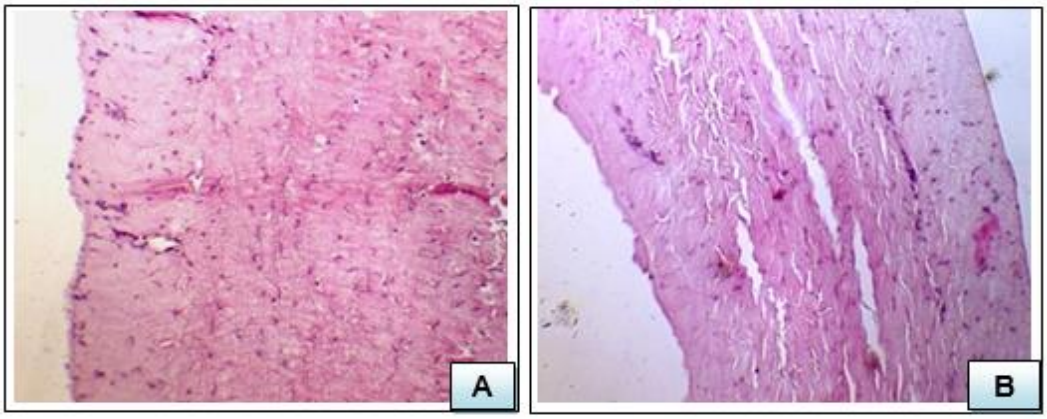

Fig 1: Histopathological section showing cellular BP (A) (H&E X100) and a cellular BP (B) (H&E X200)

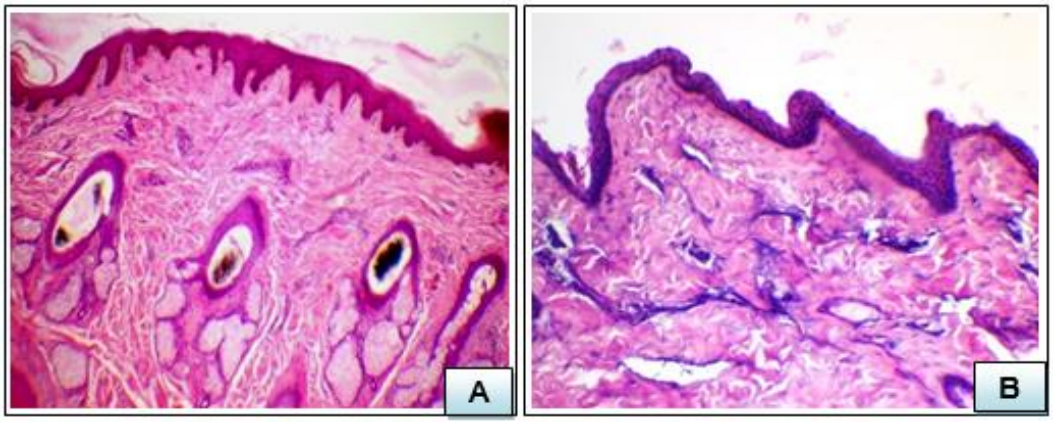

Fig 2: Histopathological section of normal bovine skin (A) (H&E 40X), The. histopathological section of acellular bovine skin showing complete loss of cellularity (B) (H&E 100 x)

Experimental design

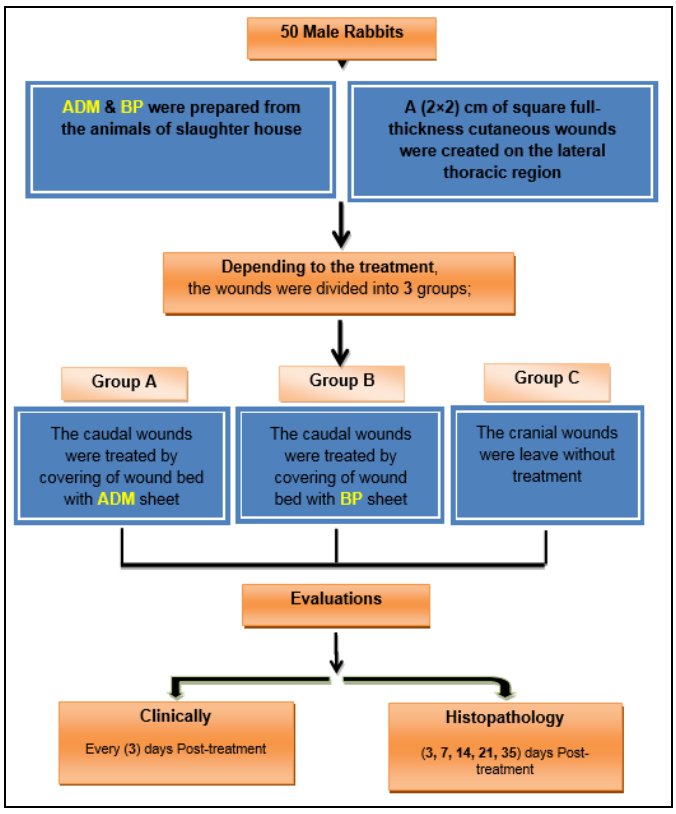

3. Results

The histopathological assessment of tissue biopsy from the wound peripheries and beds revealed that the main differences between treatment and control groups were started three days post-treatment. The histopathological sections, three day post-treatment, showed that ADM and BP scaffolds were surrounded by aggregation of intensive of inflammatory cells (Fig.3, 4). At the same period, the histopathological sections of control group were showed the presence of proliferation of blood capillaries and inflammatory cells infiltration (Fig.5). On day 7th post-treatment, the histopathological observation in control group was showed the presence of congestion blood vessels, inflammatory cells and the calcifications (Fig.6). The histopathological sections of BP-treatment group, 7th days post-treated, were showed presence of proliferation of blood capillaries and BP scaffold (Fig.7). While, in ADM-treated group on day 7th post-treated, was showed extensive infiltration of inflammatory cells with fibrosis (Fig.8). As well as, the histopathological sections of ADM-treated group were showed on day 7th post-treated, extensive infiltration of inflammatory cells between ADM scaffolds (Fig.9).

On day 14th post- wounding, the histopathological section of control group, were showed the skin consist of epidermis, dermis and regression of capillaries and high deposition of fibrous tissue (Fig.10). In (Fig.11), the histopathological section of BP-treatment group on day 14th post-treated, were showed thickening of pericardial tissue due to access of collagen fiber and less of capillaries proliferation and presence of sebaceous glands. The histopathological observation of the section of ADM-treated group, 14th days post-treatment, appeared the deposition of fibrous connective tissue (F.C.T), clear proliferation of fibroblasts and infiltration of inflammatory cells (Fig.12).

The histopathological section of control group, 21th days post-wounding, shows the epidermis and with presence of

sebaceous glands and hair follicles are absent (Fig.13). While, the histopathological sections of BP-treated group on day 21th post-treatment, were showed the restoration of epidermis with proliferation of new blood capillaries in the dermis (Fig.14). The histopathological section of ADM-treated group, 21th post-treatment, were appeared the presence of newly formed hair follicles and epidermis (Fig.15). Also, the histopathological sections of ADM-treated group were showed the presence of thick epidermal layer with deposition of F.C.T. in the dermis with the presence of fibroblasts at the same period (Fig.16).

On day 35th post-treatment, the histopathological sections of control group were confirmed the presence of collagen fibers (Fig.17). While, the histopathological sections of BP-treated wounds were showed the restoration of thin epidermal layer with a number of hair follicles (Fig.18), and the histopathological sections of ADM-treated group were appeared at the same time the aggregation of a huge infiltration of inflammatory cells and presence of lumen of hair follicles (Fig.19). As well as, the presence of sebaceous glands around hair follicles (Fig.20), associated with thickening of epidermis layer with complete and well development of hair follicles and sebaceous glands (Fig.21).

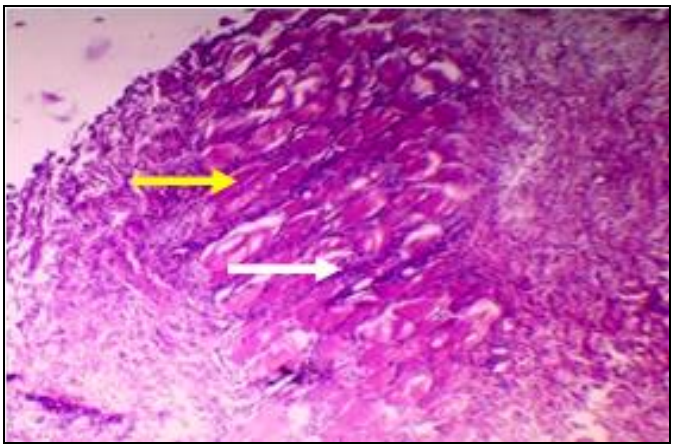

Fig 3: Histopathological section of ADM-treated group on day 3rd post-treated, shows the ADM scaffold (yellow arrow) surrounding by aggregation of intensive of inflammatory cells (white arrow) (H&E X100)

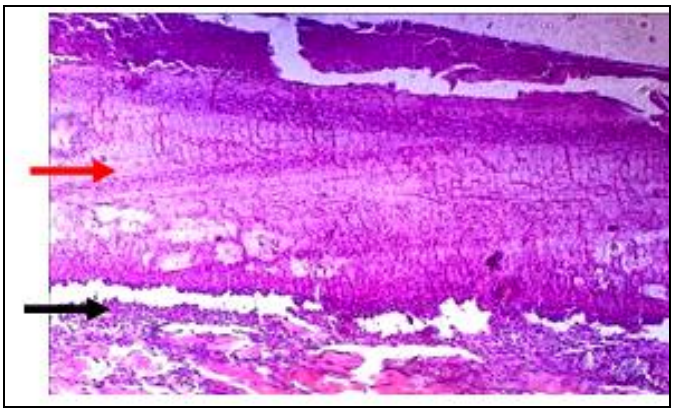

Fig 4: Histopathological section of BP-treatment group on day 3rd post-treated, shows the presence of inflammatory cells (black arrow), and BP scaffold (red arrow) (H&E X100)

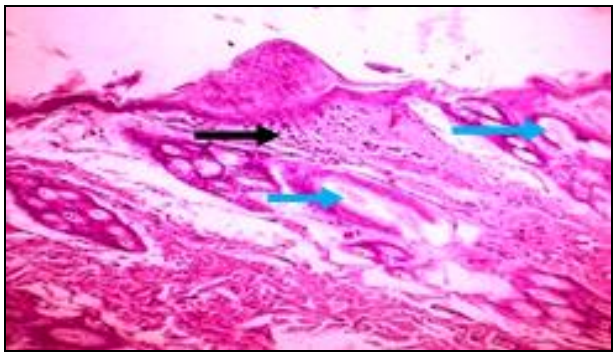

Fig 5: Histopathological section of control group on day 3rd post-wounding shows proliferation of blood capillaries (blue arrow) and inflammatory cells (black arrow) (H&E X100)

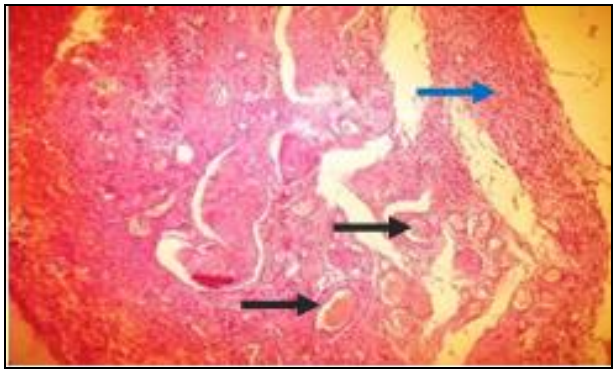

Fig 6: Histopathological section of control group on day 7th post-wounding, shows the new blood vessels (black arrow), inflammatory cells (blue arrow) and calcifications (white arrow) (H&E X100)

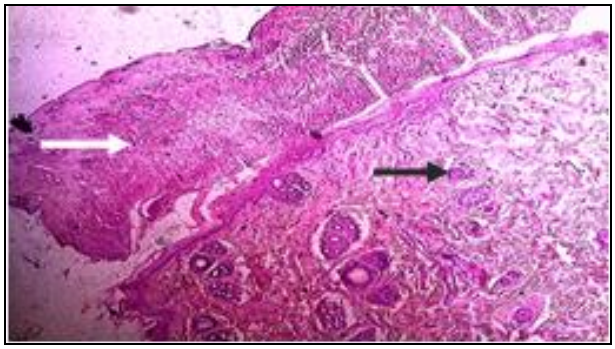

Fig 7: Histopathological section of BP-treatment group on day 7th post-treated, shows proliferation of blood capillaries (black arrow), BP scaffold (white arrow) (H&E X100)

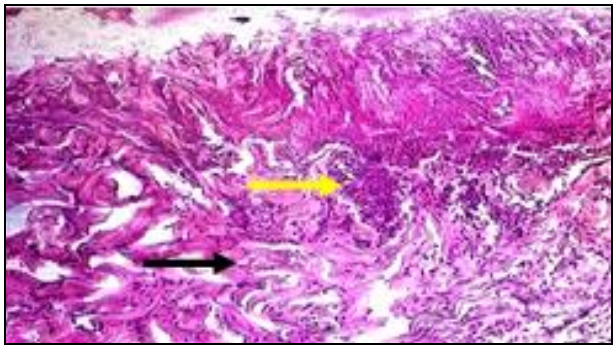

Fig 8: Histopathological section of ADM-treatment group on day 7th post-treatment, shows extensive infiltration of inflammatory cells (yellow arrow) with fibroblasts (black arrow) (H&E X100)

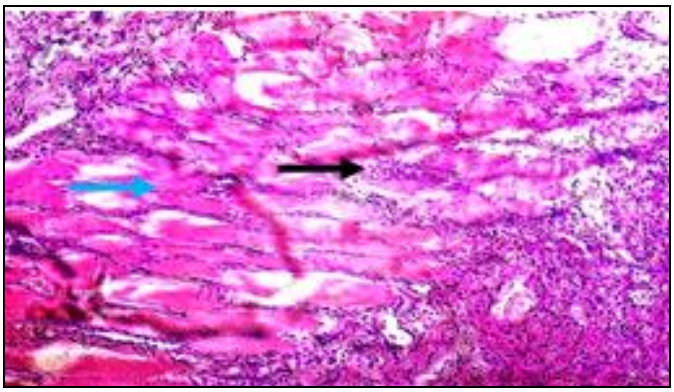

Fig 9: Histopathological section of ADM-treatment group on day 7th post-treatment, shows extensive infiltration of inflammatory cells (black arrow) within the ADM scaffold (blue arrow) (H&E X100)

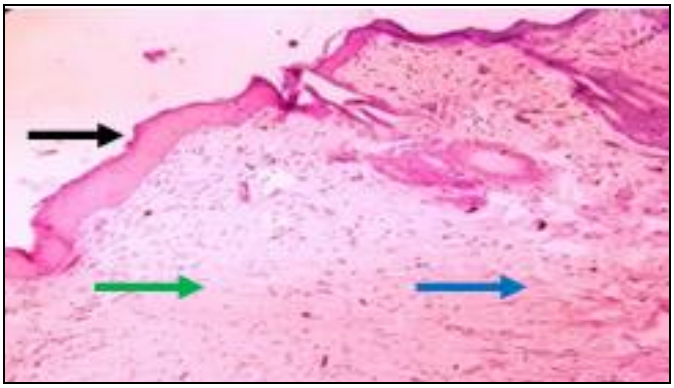

Fig 10: Histopathological section of control group, 14th days post-wounding, shows the skin consist of epidermis (black arrow), dermis (green arrow) and regression of capillaries and high deposition of fibrous tissue (blue arrow) (H&E X10)

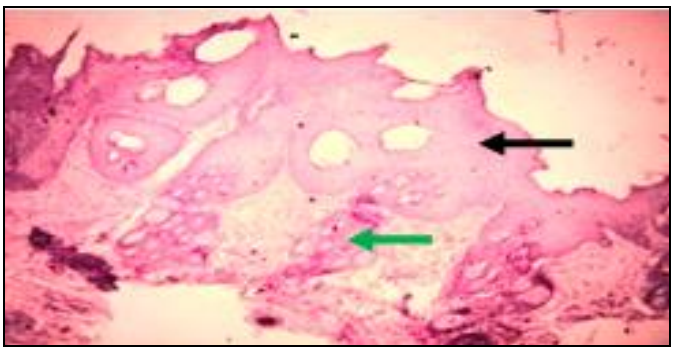

Fig 11: Histopathological section of BP-treatment group on day 14th post-treatment, shows thickening of pericardial tissue (black arrow) due to more collagen fibers and less of capillaries proliferation, presence of sebaceous gland (green arrow) (H&E 40 X)

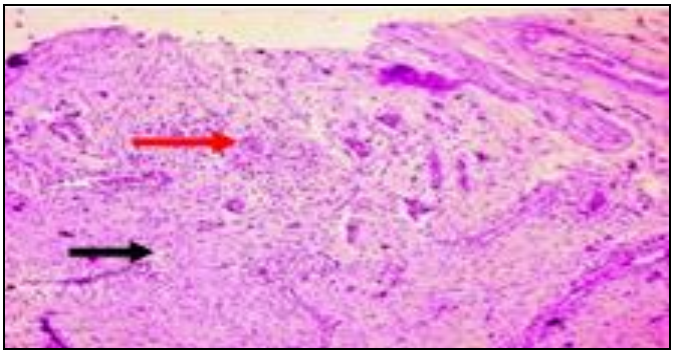

Fig 12: Histopathological section of ADM-treatment group, 14th days post-treatment, shows the deposition of fibrous tissue (black arrow), proliferation of fibroblasts and infiltration of inflammatory cells (red arrow) (H&E X100)

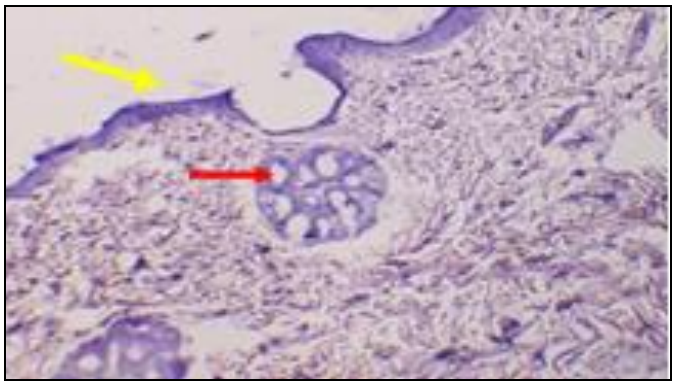

Fig 13: Histopathological section of control group, 21th days post-wounding, shows the epidermis (yellow arrow) and with presence of sebaceous glands (red arrow) and hair follicles are absent (H&E X100)

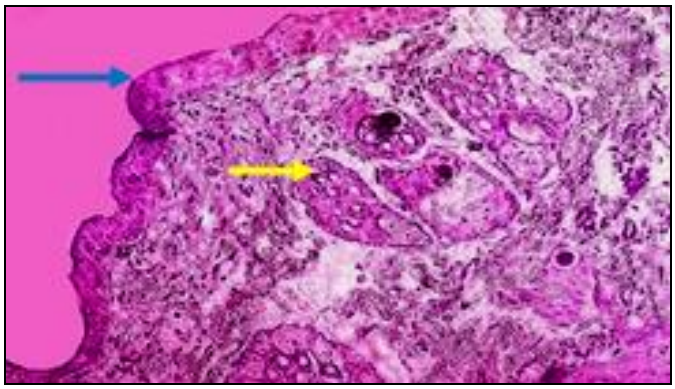

Fig 14: Histopathological section of BP-treatment group on day 21th post-treatment, shows restoration of epidermis (blue arrow) with proliferation of new blood vessels in the dermis (yellow arrow) and hair follicles are absent (H&E 40X)

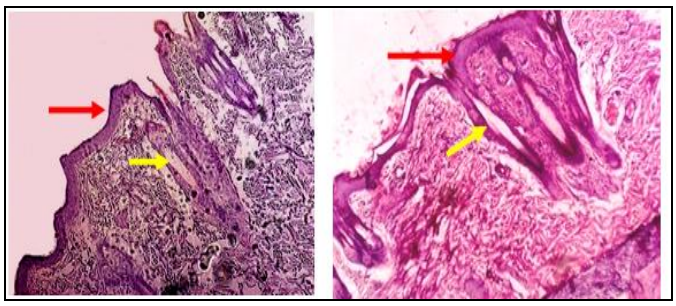

Fig 15: Histopathological section of ADM-treatment group, 21th post-treatment, shows presence of newly formed hair follicles (yellow arrow) and epidermis (red arrow) (H&E X100)

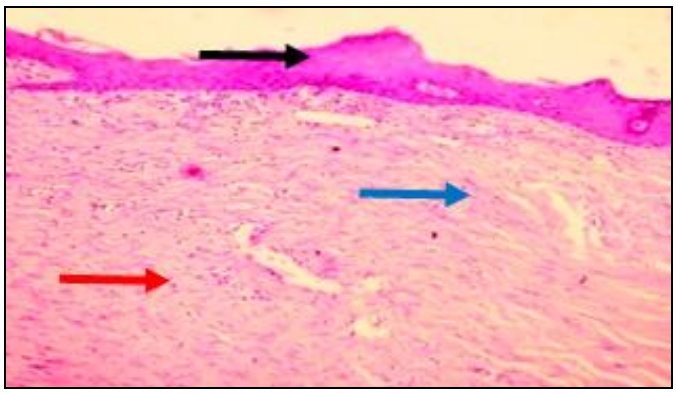

Fig 16: Histopathological section of ADM-treatment group on day 21th post-treatment, shows the presence of thick epidermal layer (black arrow) with deposition of F.C.T. in the dermis (blue arrow) with the presence of fibroblasts (red arrow) (H&E X40)

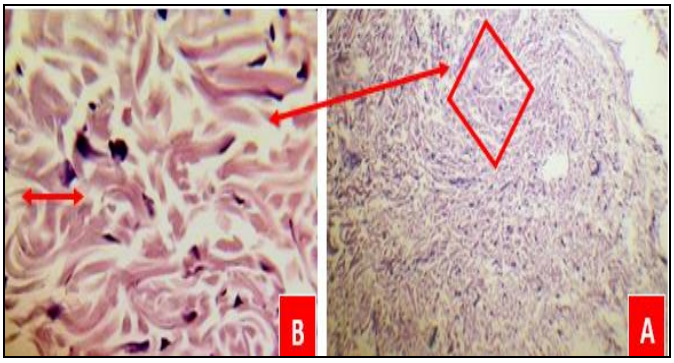

Fig 17: Histopathological section of control group on day 35th post-wounding, shows the presence of collagen fibers (red arrow) (A) (H&E X10), (B) (H&E X40)

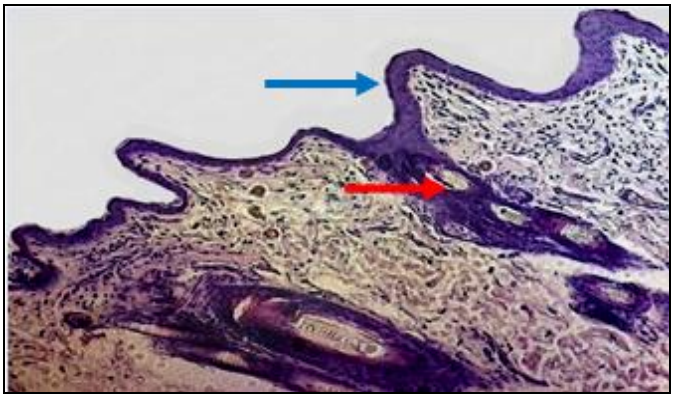

Fig 18: Histopathological section of BP-treatment group, 35th post-treatment, shows restore of thin epidermis layer (blue arrow) with number of hair follicles (red arrow) (H&E X40).

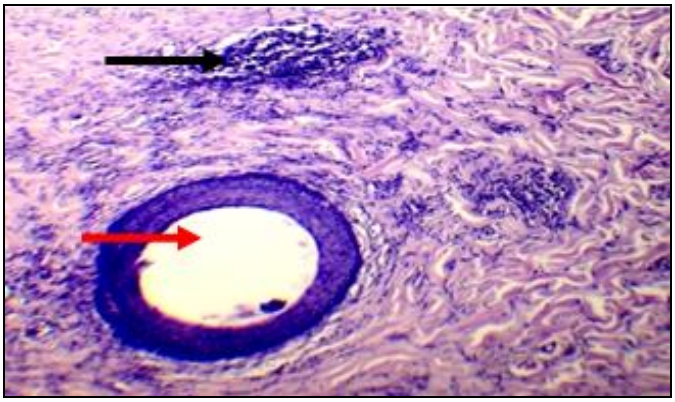

Fig 19: Histopathological section of ADM-treatment group, 35th day post-treatment, shows the aggregation of a huge infiltration of inflammatory cells (black arrow) and presence of lumen of hair follicles (red arrow) (H&E X100)

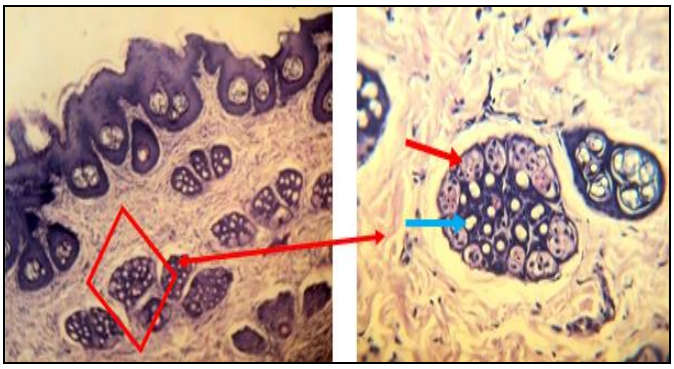

Fig 20: Histopathological section of ADM-treatment group, 35th day post-treatment, shows the presence of sebaceous glands (red arrow) around the hair follicles (blue arrow) (H&E X40)

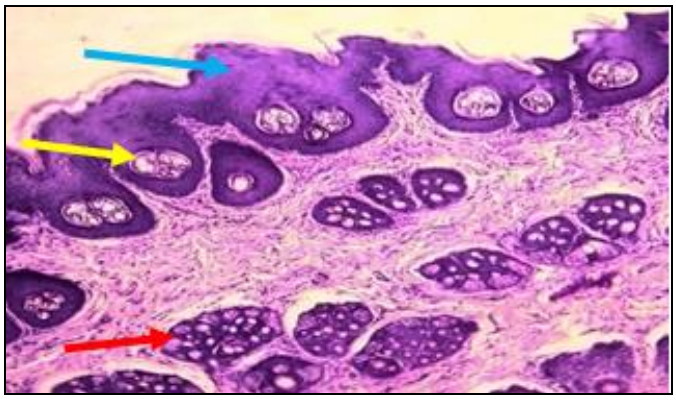

Fig 21: Histopathological section of ADM-treatment group, 35th day post-treatment, shows thick epidermis layer (blue arrow) with well development of hair follicles (yellow arrow) sebaceous gland (red arrow) (H&E X40)

4. Discussion

Full-thickness cutaneous wounds are a complete destruction of the epithelial regenerative elements that reside in the dermis and their healing occurs by granulation tissue formation, contraction and re-epithelialization [25]. The histopathological assessment of tissue biopsies from the wound peripheries and beds in the current study revealed that the main differences between treatment and control wounds were started at day 3rd post-treatment and continuous until the end of the study. The histopathological sections showed that the proliferation of blood capillaries and intensive of inflammatory cells infiltration in ADM and BP were more developed than that in control wounds which appeared in their sections. At the same time, these reactions were improved in ADM-treated wounds, in comparison to that in BP-treated wounds, along the period of the study. The histological changes were characterized by the presence of highly deposition of FCTs and infiltration of fibroblasts more than that in BP-treated wounds.

These f) on the healing of difficult to heal complex wounds, in which between years (2008-2010). They appeared that 83 wounds of 70 patients (chronic diabetic wounds, venous stasis and pressure ulcers, traumatic and surgical wounds) which were treated by application of FBDS following surgical debridement of the wounds. They submitted more than 80% of wounds underwent complete wound healing by 12 weeks after a single application of the FBDS. The scaffolds were successfully incorporated into wounds with exposed tendon or bone, and the majority of cases achieved closure through re-epithelialization by endogenous wound keratinocytes. While, [27] referred that FBDS is a bioactive collagen scaffold that assimilates into wounds and stimulates vascularization and dermal regeneration. The results of study of [28] explained, in comparative study of bovine BP and Gore-Tex in tissue interaction with wistar rats diaphragm along 21 days of the study, that histological analysis showed the presence of very limited inflammation in both BP and the diaphragm treated groups which characterized by; absence of edema, preserved blood vessels and specifically abundance of small caliber veins, indicating a possible neovascularization.

The present study showed that the degradation of both scaffolds (ADM & BP) was started at first week. The degradation process of ADM was cleared and more developed than BP due to aggregation of intensive of inflammatory cells around ADM. [14], explained that ECM scaffolds are rapidly degraded *in vivo*. They referred that 10 layer 14C-labeled ECM scaffolds were 60% degraded at 30 days post-implantation and 100% at 90 days post-surgery in a model of

canine Achilles tendon repair. During this period, the scaffold was populated and degraded by host cells and resulted in the formation of site specific functional host tissue [29]. To explain the importance of degradation process in the healing process [19], demonstrated that the degradation of ECM will lead to releasing of GFs that have been sequestered within the matrix. The presence of several GFs including; VEGF, FGF and TGF has been observed in decellularized matrix. These GFs may improve the healing reaction through the promotion of angiogenesis and other cellular responses in the local tissue environment as the ECM scaffold is naturally degraded by endogenous proteinases [30].

The histological sections in the current study were showed the incorporation of scaffolds with the host tissue, which was cleared in BP during the study. [31], studied the effects of human placenta-derived ECM containing bioactive molecules on full-thickness skin wound healing in the rat model. They referred that The ECM sheet interacted effectively and protected the wound, providing good adherence and a moist healing environment. They noticed that the ECM sheet implanted to a wound was well integrated into the host tissue within 7th days due to cellular infiltration into the sheet. As well as, [32], explained that using of BP graft for abdominal wall reconstruction even in contaminated fields, is able to resist infection after its implantation and they become completely remodeled into host tissue with mechanical and biological proprieties identical to those of the missing tissue, in addition they rapidly revascularized and maintain its original physical characteristics [33]. referred that ADM has an ability to integrate with the surrounding tissues which is less prone than synthetic materials to infection, erosion, extrusion, adhesion formation and rejection. While, [34] mentioned that after implantation of ADM into the body, it will gradually remodeled into the host tissue and revascularized. Its structural integrity is preserved and finally, it cannot be distinguished from the surrounding tissues. [35, 36] explained that when ADM is use as an implant in soft tissue procedures, appears to be fully incorporated into the wound. However, when used in a chronic wound, the matrix is eventually displaced and is not fully incorporated, associated with an excess of MMPs and reduced GFs activity. Together, these components are results during the degradation process of ECM or implants.

In general, the outcomes of the present study may related to the roles or effects of ECM bioscaffolds, including ADM and BP, on the healing process of different tissues these effects were discussed by various studies which were concluded that there are two mechanisms of actions of these bioscaffolds on the healing process of different tissues. The mechanisms of ECM scaffold-mediated constructive remodeling are not fully understood, but [37, 38] explained that the this mechanism is related to the structures and architectures of the matrices that may act as a scaffold for supporting of cells in growth and granulation tissue formation.

[39, 40] referred that ADM consist of a dermis which is a layer of the body rich with wound matrix (provides a semi-rigid elastic support system to ward off injury from trauma and provide structural and nutritional support to the epidermis layer) composed of collagen, elastin, fibrin, glycosaminoglycans (GAGs) and GFs like; FGF, PDGF and TGF. In ADM, the collagen is arranged in a reticular fashion and the scanning electron microscopic appeared that collagen fibers of ADM were orderly arranged [41]. While, BP is composed of a simple sequmous epithelium and connective tissue which is rich in collagen containing mostly collagen type-I, as well as, glycoproteins and GAGs in addition to its constitutive cells. Collagen fibers are arranged in layers with different alignment directions on each layer [42,17]. Therefore, [43] referred that the most important components of ADM & BP is collagen type-I which is stronger and more durable. Moreover, since collagen is highly hydrophilic, it can improve the interaction of cells with the scaffold. It also has the ability to trigger biological signals to support cell adhesion and proliferation. In addition, these scaffolds have receptors that permit fibroblasts, endothelial cells to attach to them, as well as, stimulate of angiogenesis. The structures of scaffolds have ability to provides a temporary supporting into which cells can migrate and proliferate in a well-organized and controlled fashion leading to improve of wound healing. In the context, [44] referred that the roughness of the biomaterial also plays an important role in the adhesion and cellular behavior and exerts direct influence both *in vitro* and *in vivo,* but the mechanisms for enhancing of cell behavior are not completely understood, but, [45] explained that the roughness of the bioscaffolds modulates the biological response of tissues to the implants.

In the study of [46], the roughness of fibrin-based dermal scaffold was estimated and clinically well established Smart Matrix® (Sa=114.776 nm). While, [47] referred that the material surface roughness has a direct influence *in vitro* as well as *in vivo* on cellular morphology, proliferation and phenotype expression. [48] added that the surface roughness can significantly increase cell migration. While, [49, 50] have demonstrated that nanometer scale of roughness has been shown to improve the adhesion and growth of both smooth muscle cells and chondrocytes on polymer scaffolds.

The literature papers have been reported that cells grown on microrough surfaces were stimulated towards differentiation; as shown by their gene expression in comparison to the cells growing on smooth surfaces. For instance, primary rat osteoblasts had higher proliferation and elevated alkaline phosphatase (ALP) activity and osteocalcin expression on the rough surface (0.81μm) in comparison with smooth one. [22] indicated that smooth surface and rough surface have different contact areas with molecules and cells and this difference in contact influences the kind of biological units' links and then conformation and function, as well as, the ability of biomaterials to incorporate to the wound bed, which promotes adhesion and migration of fibroblasts and keratinocytes. Depending on the scale of irregularities of the material surface, surface roughness can be divided to macro-roughness (100μm–milimeters) micro-roughness (100nm–100μm) and nano-roughness (less than 100 nm) each with its specific influence [51].

It's thought that the differences in pore size of each scaffold may be explained the differences in the outcomes between ADM and BP. [52, 53] mentioned that mean pore size is an essential aspect of scaffolds for tissue engineering. If pores are too small, cells cannot migrate in towards the center of the construct limiting the diffusion of nutrients and removal of waste products. Despite that pores architecture plays a vital role in the effectiveness of the scaffold; the scientific literature does not provide information about the best pores size and their distribution in the scaffold. However the relationship between scaffolds pore size and cell activity is poorly understood, as a result, there are conflicting reports within the literature on the optimal pore size required for successful tissue-engineering, nevertheless, it can be summarized that too small pores inhibit cell migration and may hinder nourishment and metabolites diffusion due to the

formation of a compact biofilm. On the other hand, too large pores may hinder cell adhesion, due to a reduced interfacial area. [54, 55] explained that cell adhesion is the binding of cells to their extracellular environment via specific ligand-integrin interactions. The results demonstrated that cell adhesion decreased with increasing pore size and that the highest levels of cell attachment were found on the scaffolds with the smallest pore size (96µm). The rationale for this result, as suggested by the authors, was the effect of specific surface area on cell adhesion due to the scaffolds with larger pores having less available specific surface area and thus a lower ligand density for initial cell attachment. In addition, [56] mentioned that the attachment of cells to large pores is limited because of the big gap to bridge between the pores.

According to the literature, the ideal pore size range for skin regeneration is 20 to 125µm [57]. Moreover, 70–110µm is regarded as the ideal pore size range for cell infiltration [57]. The study of the prosperities of two commercial type of ADM, [57] showed that both dermal scaffolds (Integra®, Smart Matrix®) have highly porous structures and have a percentage of porosity is between 80% and 90%, and both scaffolds have the majority of their pores within the ideal range for skin repair 50-100µm. Therefore, both scaffolds have the majority of their pores within the ideal range for skin repair. The bovine materials have the most open structure with porosity between the fibers, whereas the human and porcine materials are tighter and more compact. The human ADM looks slightly similar to the bovine material but with a finer texture with some minor porosity between the fibers visible. It may be a more open structure helps with the integration of the ADM material *in vivo*. This factor could be regarded a reason for improvement of cell adhesion to the ADM [57]. At the same time, [57] has estimated the pores of a cellular BP (the AGP patch) which appeared large high interconnectivity. The pore size and porosity were 159.8 m and 94.9% respectively, whereas its denaturation temperature and fixation index were 75.5°C and 57.8%, respectively (n5). While, the dermal scaffolds displayed have a very similar pore size distribution with the majority of their pores in the range of 50–100µm in size. Many mature cell types including endothelial cells (ECs) are unable to completely colonize scaffolds with the pore sizes >300µm due to the difficulty in crossing large bridging distances [58]. An "optimum pore size range" for supporting cell in growth for majority of the mature cell types, except osteoblasts and osteocytes, is in the range of 100–150µm.

The variation in the thickness of the both BP and ADM may regard as the factor which has an effects on the differences between the results of both bioscaffolds in the present study [59]. referred to that ADM thickness ranged from (0.86 to 2.18) mm (average 1.21mm), While, the thickness of BP is ranged between (0.4 and 0.7) mm [60, 61] mentioned that the thickness of scaffold materials is also important, partially for aesthetic reasons, and a thin but strong material may be desirable. Therefore, thickness normalized strength is also a useful measure of the relative merits of different materials. On a thickness-normalized scale, the fetal bovine material is the strongest and its fibers are the most oriented, which perhaps is a general feature of fetal materials and note that younger BP was found to be stronger than older [62]. The second mechanism of action of bioscaffolds on tissue healing is related to the role of their bioactive components, especially GFs, in the healing process. They have an important effect in modulating inflammatory responses, enhancing granulation tissue formation and inducing angiogenesis. They are essential for successful matrix formation and remodeling processes in the normal wound healing process. While, the deficiencies of these molecules have been reported in chronic pressure ulcers compared to the acute wounds [63, 64]. Growth factors are present within ECM in very small quantities, it act as potent modulators of cell behavior. The list of growth factors which found within ECM is extensive and includes; VEGF, FGF, PDGF, EGF, TGF, KGF, stromal-derived growth factor-1 (SDGF-1) and hepatocytes growth factor (HGF) [65, 66, 67]. These factors tend to exist in multiple isoforms, each with its specific biologic activity. Purified forms of GFs have been investigated in recent years as therapeutic methods of encouraging blood vessel formation (e.g., VEGF) stimulating deposition of granulation tissue (PDGF) and encouraging epithelialization of wounds Keratinocytes growth factors (KGF). However, this therapeutic approach has struggled because of the difficulty in determining optimal dose and methods of delivery, the ability to sustain and localize the growth factor release at the desired site and the inability to turn the factor 'on' and 'off ' as needed during the course of tissue repair [68].

Along the period of the study, no signs of immune rejection including; the signs of necrosis of the implants and prolongation of wound healing, in addition, no accumulation of inflammatory cells or immune cells (lymphocytes) were detected at the site of implantation of all treated wounds during clinical and histopathological following-up. This outcome may be related to the procedure of removing of any non-collagen components (Decellularization) from the allogeneic or xenogeneic scaffolds. Furthermore, [29] explained that post-operative inflammatory reactions are avoided with ECMs due to their cellular inert nature.

[69]. studied the immune response of the body to allogeneic and xenogeneic biologic scaffold materials. They referred that the effects of such scaffolds upon the host immune response have been largely unexplored. They concluded that the relationship between the host immune response and tissue remodeling events is a factor that logically plays, if not determinative, an important role in the successful clinical application of these devices. While, in the study of [70] to inspect the *in vivo* xenogeneic scaffold fate which is determined by residual antigenicity and ECM preservation, explained that the reduction of both hydrophilic and lipophilic antigens with stepwise, solubilization-based antigen removal is critical to decreased *in vivo* immune response towards BP implants. Promotion of lipophile solubilization following hydrophile solubilization substantially reduced local innate, local cell-mediated adaptive, local humeral-mediated adaptive and systemic humeral immune responses beyond that achieved by hydrophile solubilization alone [71]. explained that the effective removal of the cell population clears donor antigens, reduces the possibilities of *in vitro* cytocompatibiltiy and *in vivo* adverse host response, thus helping to avoid potential pro-inflammation response and immune rejection in the recipient [72]. They referred to the ADM with normal collagen bundling and organization and an intact basement membrane complex was obtained from human cadaveric skin, and its clinical application led to sufficient host cell infiltration and neovascularization, with undetectable immune response [73]. In addition, [74, 75] explained that the surface characteristics of biomaterial and its composition may affect the course and the extent of the immune reaction. Flat and smooth surfaces generally lead to the formation of fibrosis, whereas, implants with a rough surface, such as vascular prostheses, become covered by a layer of macrophages and giant cells with variable amounts of granulation tissue which

can persist around the implant and potentially isolate it from the local tissue. At the same time, they referred that natural biomaterials which including; collagen, fibrinogen, hyaluronic acid (HA) GAGs, hydroxyapatite, chitosan, silk or starch, mimic ECM components may be make them less immunogenic. They can, however, also trigger an immune response, causing monocytes to release IL-1B and IL-6 [76]. Various types of cells, including macrophages, T-cells, fibroblasts, keratinocytes, and endothelial cells, produce IL-6, which exhibits various activities on a wide variety of cells including lymphocytes, hepatocytes, and neuronal cells.

5. Conclusions

1. The chemical decellularization of ADM and BP scaffolds appears to be an effective technique for producing of cell-free structures and avoiding of immune-rejection of bio-implants.
2. Both acellular ADM and BP can be used for acceleration and enhancement of full-thickness cutaneous wounds healing with the superiority of ADM than BP implants.

6. Acknowledgments.

In the name of Allah the Merciful. I would like to thank all members and staff of department of Surgery and Obstetric in the College of Veterinary Medicine, University of Baghdad, Iraq, whom were involved in this study.

7. References

1. Shakya P, Sharma AK, Kumar N, Vellachi R, Mathew DD, Dubey P, *et al*. Bubaline Cholecyst Derived Extracellular Matrix for Reconstruction of Full Thickness Skin Wounds in Rats. Scientifica. vol. 2016, Article ID 2638371, 13 pages, 2016. doi:10.1155/2016/2638371
2. Guo S, Dipietro LA. Factors Affecting Wound Healing. J. Dent. Res., 2010; 89(3):219-229.
3. Eming SA, Martin P, Tomic-Canic M. Wound repair and regeneration: mechanisms, signaling, and translation. Sci. Transl. Med., 2014; 6:265-266.
4. Ojeh N, Pastar I, Tomic-Canic M, Stojadinovic O. Stem Cells in Skin Regeneration, Wound Healing, and Their Clinical Applications. Int. J Mol. Sci., 2015; 16:25476-25501
5. Carter JM, Tingley-Kelley K, Warriner IRA. Silver treatments and silver-impregnated dressings for the healing of leg wounds and ulcers: A systematic review and meta-analysis. J Am. Acad. Dermatol., 2010; 63:668-679.
6. Amsler F, Willenberg T, Blättler W. In search of optimal compression therapy for venous leg ulcers: A meta-anlysis of studies comparing divers bandages with specially designed stockings J. Vasc. Surg., 2009; 50:668–674.
7. Cullum, N.A.; Al-Kurdi, D.; Bell-Syer, S.E. Therapeutic ultrasound for venous leg ulcers. Cochrane Database Syst. Rev., 2010; 16(6):doi:10.1002/14651858.CD001180.pub3.
8. Armstrong, D.G.; Marston, W.A.; Reyzelman, A.M.; Kirsner, R.S. Comparison of negative pressure wound therapy with an ultraportable mechanically powered device vs. traditional electrically powered device for the treatment of chronic lower extremity ulcers: A multicenter randomized- controlled trial. Wound Repair Regen., 2011; 19:173–180.
9. Dumville JC, Worthy G, Soares MO, Bland JM, Cullum N, Dowson C, *et al*. A randomised controlled trial of larval therapy in the management of leg ulcers. Health Technol. Assess., 2009; 13:1-206.
10. Greaves NS, Benatar B, Baguneid M, Bayat A. Single-stage application of a novel decellularized dermis for treatment-resistant lower limb ulcers: Positive outcomes assessed by SIA scopy, laser perfusion, and 3D imaging, with sequential timed histological analysis. Wound Repair Regen. 2013; 21:813-822.
11. Sara U, Bayat A. Electrical Stimulation and Cutaneous Wound Healing: A Review of Clinical Evidence. J health care. 2014; 2:445-467.
12. Turner NJ, Badylak SF. The Use of Biologic Scaffolds in the Treatment of Chronic Non healing Wounds. Adv. Wound Care. 2014; 4(8):490-500.
13. AL-Bayati AHF, AL-Tememe HAK, AL-Mudallal NHA. Role of a cellular bovine urinary bladder submucosa on skin wound healing in Iraqi goats. The Iraqi Journal of Veterinary Medicine. 2016; 40(1):53-60.
14. Brown S, Badylak SF. An acellular biologic scaffold promotes skeletal muscle formation in mice and humans with volumetric muscle loss, Science Translational Medicine. 2014; 6(234):234-458.
15. Kumar N, Purohit S, Sharma AK, Sharma AK. Development of Acellular Dermal Matrix from Skin of Different Species of Animals Using Biological Detergents and Enzymes Combinations. J.S.M. Burns Trauma. 2016; 1(1):1004.
16. Ott HC, Clippinger B, Conrad C, Schuetz C, Pomerantseva I, Ikonomou L, *et al*. Regeneration and orthotopic transplantation of a bioartificial lung. Nat. Med., 2010; 16:927-933.
17. Athar Y, Zainuddin SLA, Berahim Z, Hassan A, Sagheer A, Alam MK. Bovine Pericardium: A Highly Versatile Graft Material. International Medical Journal. 2014; 21(3):321-324.
18. Shukla A, Nandi P, Ranjan M. Acellular Dermis as a Dermal Matrix of Tissue Engineered Skin Substitute for Burns Treatment. Ann. Public Health Research. 2015; 2(3):1023.
19. Swinehart IT, Badylak SF. Extracellular Matrix Bioscaffolds in Tissue Remodeling and Morphogenesis. Development Dynamics. 2016; 245:351-360.
20. Brennan EP, Reing J, Chew D, Myers-Irvin JM, Young EJ, Badylak SF. Antibacterial activity within degradation products of biological scaffolds composed of extracellular matrix. Tissue Eng., 2006; 12(10):2949-2955.
21. Freytes DO, Stoner RM, Badylak SF. Uniaxial and biaxial properties of terminally sterilized porcine urinary bladder matrix scaffolds, Journal of Biomedical Materials Research Part B: Applied Biomaterials. 2008; 84(2):408-414.
22. Kumar AB, Kumar S, Kumar AS, Kumar N, Kumar SM. Effect of Bovine Collagen Sheet with Fibroblast Cell in full Thickness Skin Wound Healing in Rat Model. Research Journal for Veterinary Practitioners. 2014; 2(5):91-97.
23. Luna LG. Histopathologic methods and color atlas of special stains and tissue artifacts. Maryland: American Histolabs. Inc. 1992.
24. SAS. Statistical Analysis System, User's Guide. Statistical. Version 7th ed. SAS. Inst. Inc. Cary. N.C. USA. 2004
25. Hasana A, Kumara N, Gopinathana A, Singha K, Sharmaa AK, Remyaa V, *et al*. Bovine reticulum derived

extracellular matrix (b-REM) for reconstruction of full thickness skin wounds in rats. Original Research Article, Wound Medicine. 2016; 12:19-31.
26. Strauss NH, Brietstein RJ. Fetal Bovine Dermal Repair Scaffold Used for the Treatment of Difficult-to-Heal Complex Wounds. Wounds. 2012; 24(11):327-334.
27. Parcells AL, Karcich J, Granick MS, Marano MA. The Use of Fetal Bovine Dermal Scaffold (PriMatrix) in the Management of Full-Thickness Hand Burns. Eplasty. 2014; 14:e36.
28. Guerra AF, Filho MR, Novo NF, França WM. Comparative Study of Bovine Pericardium and Gore-Tex in Tissual Interaction with Wistar Rats Diaphragm. Surgical Science. 2016; 7:381-389.
29. Gilbert TW, Stewart-Akers AM, Simmons-Byrd A, Badylak SF. Degradation and remodeling of small intestinal submucosa in canine Achilles tendon repair. J Bone Joint Surg. Am., 2007; 89:621-30.
30. Reing JE, Brown BN, Daly KA, Freund JM, Gilbert TW, Hsiong SX, *et al*. The effects of processing methods upon mechanical and biologic properties of porcine dermal extracellular matrix scaffolds. Biomaterials. 2010; 31:8626-8633.
31. Choi JS, Kim JD, Yoon HS, Cho YW. Full-thickness skin wound healing using human placenta-derived extracellular matrix containing bioactive molecules. Tissue Eng. Part A. 2013; 19:329-339.
32. D'Ambra L, Berti S, Feleppa C, Magistrelli P, Bonfante P, Falco E. Use of bovine pericardium graft for abdominal wall reconstruction in contaminated fields. World J. Gastrointest. Surgery. 2012; 4(7):171-176.
33. Zhong T, Janis JE, Ahmad J, Hofer SO. Outcomes after abdominal wall reconstruction using a cellular dermal matrix: a systematic review. J Plast. Reconstr. Aesthet. Surg., 2011; 64:1562-1571.
34. Song Z, Yang Z, Yang J, Liu Z, Peng Z, Tang R, Gu Y. Repair of Abdominal Wall Defects In Vitro and In Vivo Using VEGF Sustained-Release Multi-Walled Carbon Nanotubes (MWNT) Composite Scaffolds. PLoS One. 2013; 8(5):e64358.
35. Mulder G, Lee DK. A retrospective clinical review of extracellular matrices for tissue reconstruction: equine pericardium as a biological covering to assist with wound closure. Wounds. 2009; 21(9):254-61.
36. Ching YH, Sutton TL, Pierpont YN, Robson MC, Payne WG. The use of growth factors and other humoral agents to accelerate and enhance burn wound healing. Eplasty. 2011; 11:e41.
37. Zajicek R, Mandys V, Mestak O, Sevcik J, onigova RK, Matouskova E. Human keratinocytes growth and differentiation on acellular porcine dermal matrix in relation to wound healing potential, The Scientific World J, Article ID 727352, 8 Pages. 2012
38. Canonico S, Campitiello F, Della Corte A, PadovanoV, Pellino G. Treatment of Leg Chronic Wounds with Dermal Substitutes and Thin Skin Grafts. Skin Grafts. 2013; Chapter5, :51-76.
39. Perumal S, Antipova O, Orgel JP. Collagen fibril architecture, domain organization, and triple-helical conformation govern its proteolysis. Proc. Natl. Acad. Sci. USA. 2008; 105:2824.
40. Fosnot J, Kovach SJ, Serletti JM. Acellular Dermal Matrix: General Principles for the Plastic Surgeon. Aesthetic Surgery Journal. 2011; 31(7S):5S-12S.
41. Luo X, Xin GH, Zeng TF, Lin C, Zeng YL, Li YC, *et al*. Effects of microporous porcine acellular dermal matrix combined with bone marrow mesenchymal cells of rats on the regeneration of cutaneous appendages cells in nude mice. Zhonghua Shao Shang Za Zhi. 2014; 29(6):541-547.
42. Daar E, Woods E, Keddie JL, Nisbet A, Bradley DA. Effect of penetrating ionizing radiation on the mechanical properties of pericardium, Nucl. Instrum. Methods Phys. Research. 2010; 619:356-360.
43. Jackson CJ, Xue M. Extracellular Matrix Reorganization During Wound Healing and Its Impact on Abnormal Scarring. Adv. wound care. 2014; 4:119-136.
44. Santos VD, Brandalise RN, Savaris M. Biomaterials: Characteristics and Properties. Topics in Mining, Metallurgy and Materials Engineering. Springer, Cham. 2017, 5-15.
45. Mondalek FG, Lawrence BJ, Kropp BP, Grady BP, Fung KM, Madihally SV, *et al*. The incorporation of poly (lactic-co-glycolic) acid nanoparticles into porcine small intestinal submucosa biomaterials. Biomaterials. 2008; (29):1159-66.
46. Sharma V, Patel N, Kohli N, Ravindran N, Hook L, Mason C, *et al*. Viscoelastic, physical, and bio-degradable properties of dermal scaffolds and related cell behavior. Biomed. Mater., 2016; 11(5):055001.
47. Hatano K, Inoue H, Kojo T, Tsujisawa T, Uchiyama C, Uchida Y. Effect of Surface Roughness on Proliferation and Alkaline Phosphatase Expression of Rat Calvarial Cells Cultured on Polystyrene. Bone. 1999; 25:439-445.
48. Lampin M, Warocquier C, Legris C, Degrange M, Sigot Luizard MF. Correlation between substratum roughness and wettability, cell adhesion, and cell migration. J Biomed. Mater. Research. 1997; (36):99-108.
49. Park GE, Pattison MA, Park K, Webster TJ. Accelerated chondrocyte functions on NaOH treated PLGA scaffolds. Biomaterials. 2005; (26):3075-82.
50. Pattison MA, Wurster S, Webster TJ, Haberstroh KM. Three-dimensional, nano-structured PLGA scaffolds for bladder tissue replacement applications. Biomaterials. 2005; (26):2491-500.
51. Agaska B, Bacakova L, Filova E, Balik K. Osteogenic Cells on Bio- Inspired Materials for Bone Tissue Engineering. Physiological Research. 2010; 59:309-322.
52. Harley BA, Kim HD, Zaman MH, Yannas IV. Lauffenburger DAGibson, LJ. Microarchitecture of three-dimensional scaffolds influences cell migration behavior via junction interactions. Biophys J., 2008; 95:4013-24.
53. Ciara MM, O'Brien FJ. Understanding the effect of mean pore size on cell activity in collagen-glycosaminoglycan scaffolds. Cell Adhesion and Migration. 2010; 4 (3):377-381.
54. O'Brien FJ, Harley BA, Yannas IV, Gibson LJ. The effect of pore size on cell adhesion in collagen-GAG scaffolds. Biomaterials. 2005; (26):433-41.
55. O'Brien FJ, Harley BA, Waller MA, Yannas IV, Gibson LJ. The effect of pore size on permeability and cell attachment in collagen scaffolds for tissue engineering. Technol. Health Care. 2007; 15:3-17.
56. Wolf K, Alexander S, Schacht V, Coussens LM, von Andrian UH, van Rheenen J, *et al*. Collagenbased cell migration models in vitro and in vivo. Semin. Cell Dev. Biol., 2009; 20(8):931-941.
57. Ikada Y. Tissue Engineering: Fundamentals and Applications (UK: Academic Press). 2011
58. Wang YC. Micropatterning of proteins and mammalian

cells on biomaterials. Faseb. J, 2004; (18):525-7.
59. Rose JF, Zafar SN, Ellsworth WA. Does Acellular Dermal Matrix Thickness Affect Complication Rate in Tissue Expander Based Breast Reconstruction?. Plastic Surgery International. 2016; Article ID 2867097, 6.
60. Biellia A, Bernardinib R, Varvarasc D, Rossic P, Blasid G, Petrellac G, Buonomoc OC, *et al*. Characterization of a new decellularized bovine pericardial biological mesh: Structural and mechanical properties. J of the Mechanical Behavior of Biomedical Materials. 2018; 78:420-426.
61. Wells HC, Sizeland KH, Kirby N, Hawley A, Mudie S, Haverkamp RG. Collagen Fibril Structure and Strength in Acellular Dermal Matrix Materials of Bovine, Porcine, and Human Origin. ACS Biomater. Sci. Eng., 2015; 1:1026-1038.
62. Sizeland KH, Wells HC, Higgins JJ, Cunanan CM, Kirby N, Hawley A, Haverkamp RG. Age dependent differences in collagen fibril orientation of glutaraldehyde fixed bovine pericardium. BioMed. Res. Int., 2014; 189197.
63. Cooper DM, Yu EZ, Hennessey P, Ko F, Robson MC. Determination of endogenous cytokines in chronic wounds. Ann. Surg., 1994; (219):688-692.
64. Pierce GF, Tarpley JE, Tseng J, Bready J, Chang D, Kenney WC, *et al*. Detection of platelet-derived growth factor (PDGF)-AA in actively healing human wounds treated with recombinant PDGF-BB and absence of PDGF in chronic nonhealing wounds. J Clin. Investig. 1995; (96):1336.
65. Bonewald LF. Regulation and regulatory activities of transforming growth factor. Critical Reviews in Eukaryotic Gene Expression. 1999; 9(1):33-44.
66. Kagami S, Kondo S, Loster K, Reutter W, Urushihara M, Kitamura A, Kobayashi S, Kuroda Y. Collagen type I modulates the platelet-derived growth factor (PDGF) regulation of the growth and expression of β1integrins by rat mesangial cells. Biochemical & Biophysical Research Communications. 1998; 252(3):728-732.
67. Roberts R, Gallagher J, Spooncer E, Allen TD, Bloomfield F, Dexter TM. Heparan sulphate bound growth factors: a mechanism for stromal cell mediated haemopoiesis. Nature. 1988; 332(6162):376-378.
68. Badylak S, Gilbert T, Myers-Irvin J. The extracellular matrix as a biologic scaffold for tissue engineering. Tissue Engineering. 2008, 121-143.
69. Badylak SF, Gilbert TW. Immune Response to Biologic Scaffold Materials. N.I.H. Public Access, semin. immunol. 2008; 20(2):109-116.
70. Wong ML, Wong JL, Vapniarsky N, Griffiths LG. In vivo xenogeneic scaffold fate is determined by residual antigenicity and extracellular matrix preservation. Biomaterials. 2017; 92:1-12.
71. Yi S, Ding F, Gong L, Gu X. Extracellular Matrix Scaffolds for Tissue Engineering and Regenerative Medicine. Curr. Stem Cell Res. & Ther., 2017; 12(3):233-246.
72. Rana D, Zreiqat H, Benkirane-Jessel N, Ramakrishna S, Ramalingam M. Development of decellularized scaffolds for stem cell driven tissue engineering. J Tissue Eng. Regen. Med. 2015; 11(4):942-965.
73. Wainwright DJ. Use of an acellular allograft dermal matrix (AlloDerm) in the management of full-thickness burns. Burns. 1995; 21(4):243-8.
74. Velnar T, Bunc G, Klobucar R, Gradisnik L. Biomaterials and host versus graft response: a short review, Bosn. J Basic Med. Sci., 2016; 16:82-90.
75. Cravedi P, Farouk S, Angeletti A, Edgar L, Tamburrini R, Dusuit J, *et al*. Regenerative Immunology: The Immunological Reaction to Biomaterials. Transpl. Int. 2017; 30:1199-1208. doi:10.1111/tri.13068
76. Rayahin JE, Gemeinhart RA. Activation of Macrophages in Response to Biomaterials. Results Probl. Cell Differ. 2017; 62:317-351.